**ANALYSES OF RIDGES ON ENCELADUS FROM LIMB PROFILES AND ADDITIONAL TECHNIQUES.** H. Chilton[1,2], D. A. Pathoff[2], R. Pappalardo[2] and P. Thomas[3]. [1]Geology and Physics, California State University – Fullerton, 800 N. State College Blvd., Fullerton, CA 92831-3599, [2]Jet Propulsion Laboratory, California Institute of Technology, 4800 Oak Grove Drive, Pasadena, CA 91109, [3]Center for Radiophysics and Space Research, Cornell University, Ithaca, NY 14853.

**Introduction:** Deformation of icy satellites often takes the form of ridge and trough terrains. However, the mechanisms for their development are poorly constrained or understood but likely offer key insights into the local and regional deformational history [1-3]. Using Cassini's rich Imaging Science Subsystem (ISS) data set, we use limb profiles, stereo-maps, and supporting images to characterize the morphologies of ridges in various regions of Enceladus, including the leading hemisphere (LH), trailing hemisphere (TH), Samarkand region, and the south polar terrain (SPT). The ridges in the northern portion of the LH have been roughly characterized as ridge-and-trough terrain while to the south the terrain have been categorized as striated ridge-and-trough terrain [4]. Tilted ice blocks have been suggested to form the ridges in the Samarkand region [1]. The large fractures of the STP, known as "Tiger Stripes," have been described as ~500 m deep troughs with 100-200 m high raised flanks and are the source of water plumes emanating from the moon's surface [5-7]. We use limb profiles complemented with additional methods that includes incidence and emission angle derived critical slope angles and average slope angles to further characterize ridges on Enceladus.

**Methods:** Here we emphasize limb derived elevation profiles, while also utilizing other methods to best constrain and characterize morphology.

*Limb profiles.* Elevation profiles are derived from higher resolution limb images than previously used [8] so as to extract local topography. Images have also been generally selected for those with ridges and structures that are near-orthogonal to the limb. Sub-pixel resolution from the derivation algorithm equates to tens of meters vertically and horizontally, providing extremely fine line-of-sight profiles of ridges and other landforms in the derived profile "skyline." Several challenges exist for limb profiles that require particular care when being used for analysis: 1) Limb profiles are a topographic sum along a line-of-sight, and can include foreground and background features, 2) features composing the skyline can be misidentified, and 3) ridges in profile only show slope minimums. Although only minimums, these slopes can still be roughly representative of the ridge slope and can be substantiated using additional methods. Where distinct ridge trends are observed, corrections of apparent to actual slope angle can be made.

*Incidence and emission derived critical slope angles.* The complement of the incidence angle represents a critical angle, where any slope shallower than this, will not cast a shadow while anything steeper will cast a shadow. Similarly, if a slope is lit and visible, the complement of the emission angle represents the maximum slope angle. These values help constrain and evaluate slope angles determined in limb profiles.

*Average slope angles.* For instances where a ridge crest is identifiable but portions of the slope are obscured, an average slope angle can be derived. We use the height determined in the limb derived profile and measure the distance from the crest to the base to calculate the average slope angle.

*Stereo profiles.* We will be considering stereo data in future work. Combined with the high resolution limb profiles, this data will provide a large and detailed data set of ridge cross-sections and local topography.

**Results:** In addition to characterization of ridges, we are able to evaluate the methodology used in this project. Derived limb profiles provide highly detailed results with insights into local feature comparisons, individual feature characteristics, and in particular extremely accurate ridge heights; with smaller scale analyses it does become important to include additional methods to complement the derived values.

*Leading Hemisphere, Northern Ridges.* Ridges in the northern portion of the LH (the LH smooth unit of [4]) commonly have rounded crests with profile slopes between 6° and 30°. Some of these ridges also have wrinkled appearances, such as seen in Fig 1, with variability in shadows, shading, and lit portions indicating notable changes in slope. Incidence-angle derived slopes require greater than 67° slopes for this area in order to cast true shadows in the image shown in Fig 1. Comparatively, the average limb-derived slope angle is

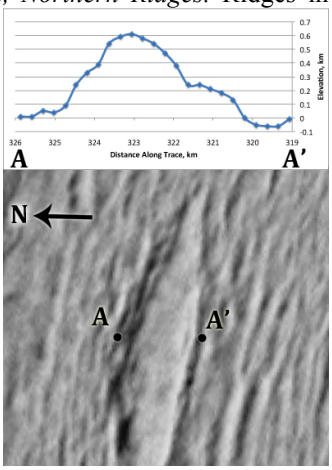


Fig 1. Leading Hemisphere, North. Limb derived elevation profile from A-A' from Cassini ISS limb image N1669819341.

20°. These wide variations in slope angles are consistent with their convoluted and wrinkled appearance.

*Leading Hemisphere, Southern Ridges.* In the southern portion of the LH (the central LH unit from [4]), two cratered islands are bounded by younger terrains to the north and south (Fig 2). To the north of

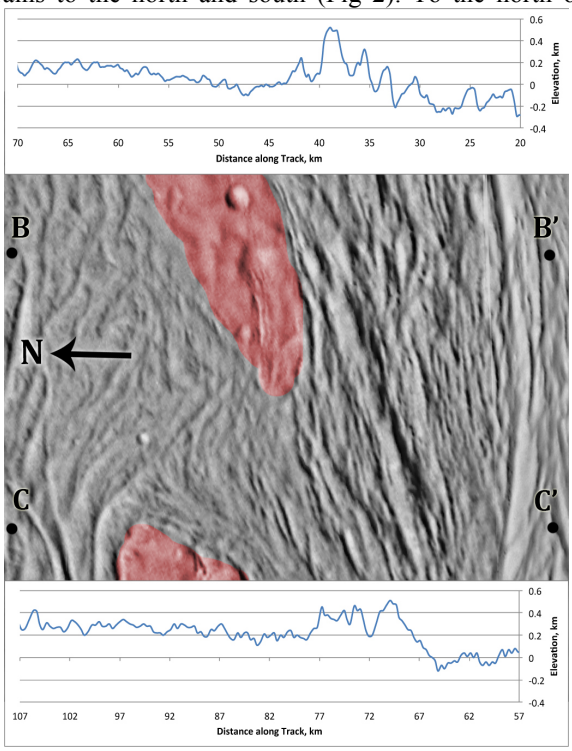


Fig 2. Leading Hemisphere, South. The cratered 'islands' are highlighted in red and two profiles show the shallow ridges to the north and the tall, angular ridges to the south.

these cratered islands are rounded ridges 100-200 m in height, with limb-derived profile slopes of 4° to 11°. These ridges also sit at average elevations (100-200 m) higher than either the cratered islands or the taller, prominent ridges farther south. The ridges south of the cratered islands have limb-derived ridge slopes up to 42° and are 200-500 m high. Incidence-angle derived slopes are 53° to 58°. No distinct slope breaks or shallowing is measured.

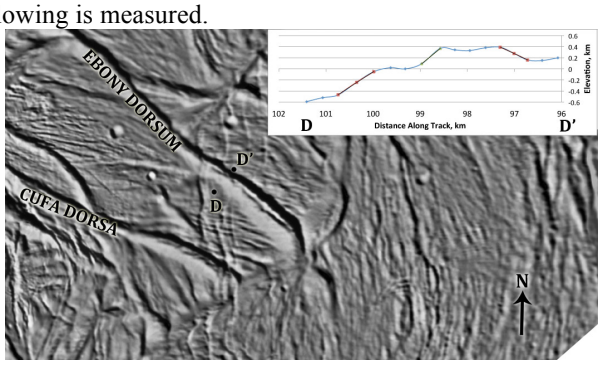


Fig 3. Dorsa of the Trailing Hemisphere with smaller ridges visible along the right edge of the image.

*Ridged Unit of the Trailing Hemisphere.* Prominent ridges in the TH vary ranging from the 200-400 m high ridges towards the boundary of this region, to the large, prominent Dorsa that occur in the central area. These large single ridges, including Ebony Dorsum and Cufa Dorsa, reach almost 1 km in height and show limb-derived slopes around 35°. These angles contrast with a ridge north of Ebony Dorsum that is 400 m high and shows a distinct 16° upper slope and a 5° basal slope. Detailed description and analysis is described in [9].

*Samarkand region.* Fig 4 shows a ridged portion of the Samarkand Sulci with a distinct trough bounded on the west by an asymmetrical ridge. The west-facing slope reaches 11° in the limb-derived profile, with the upper and lower eastern facing slopes reaching 24° and 34° respectively.

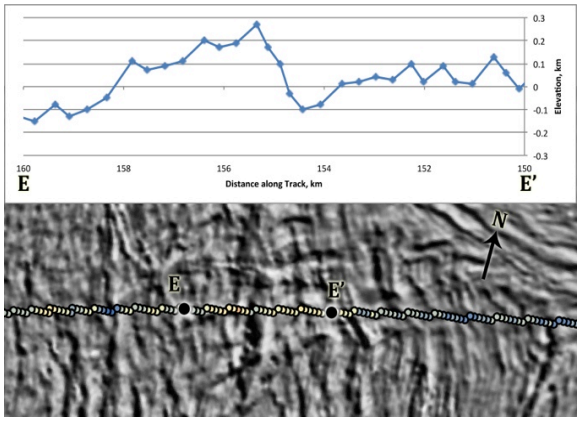


Fig 4. Samarkand region with a of section of the profile from E-E' showing distinct angles between the two sides of the central ridge.

*South Polar Terrain.* Limb-derived elevation profiles in the SPT indicate the tiger stripe ridges are 70 to 120 m high from crest to base for Baghdad and Damascus. Relative to the surrounding terrain, the ridges reach 160 to 190 m for Baghdad and 160 to 210 m for Damascus. Limb-derived slopes reach 23° but are commonly less than 10°.

**References:**

[1] Kargel, J.S. and Pozio, S. (1996) *Icarus, 119:2,* 385-404. [2] Geissler, P.S. et al. (1998) *Icarus, 135:*1, 107-126. [3] Pappalardo, R.T. and Greeley, R. (2006) *JGR, 100:E9,* 18,985-19,007. [4] Crow-Willard, E.N., and Pappalardo, R.T. (2010) *LPSC XLI,* Abstract #2715. [5] Porco, C.C., et al. (2006) *Science, 331,* 1393-1401. [6] Procter, L.M., et al. (2010) *Space Sci Rev, 153:*63-111. [7] Spencer, J.R. and Nimmo, F. (2013) *Annu. Rev. Earth Planet. Sci. 41,* 693-717. [8] Nimmo, F., et al. (2011) *LPSC XLII,* Abstract #1523. [9] Pappalardo, R.T. et al. (2014) *LPSC XLV,* Abstract #2143